International Journal for Parasitology 52 (2022) 677–689

Contents lists available at ScienceDirect

International Journal for Parasitology

journal homepage: www.elsevier.com/locate/ijpara

Genomic signatures of selection associated with benzimidazole drug treatments in *Haemonchus contortus* field populations

Janneke Wit [a,b,*], Matthew L. Workentine [a], Elizabeth Redman [a], Roz Laing [c], Lewis Stevens [d], James A. Cotton [e,1], Umer Chaudhry [f,2], Qasim Ali [g], Erik C. Andersen [h], Samuel Yeaman [i], James D. Wasmuth [a,b], John S. Gilleard [a,b,*]

[a] *Faculty of Veterinary Medicine, University of Calgary, Calgary, Alberta, Canada*
[b] *Host-Parasite Interactions (HPI) Program, University of Calgary, Calgary, Alberta, Canada*
[c] *Institute of Biodiversity Animal Health and Comparative Medicine, College of Medical, Veterinary and Life Sciences, University of Glasgow, Garscube Campus, Glasgow, UK*
[d] *Tree of Life, Wellcome Sanger Institute, Cambridge, UK*
[e] *Wellcome Sanger Institute, Wellcome Genome Campus, Hinxton, Cambridgeshire, UK*
[f] *University of Edinburgh, Roslin Institute, Easter Bush Veterinary Centre, Roslin, Midlothian, UK*
[g] *Department of Parasitology FVAS, University of Agriculture, D.I. Khan, Pakistan*
[h] *Molecular Biosciences, Northwestern University, Evanston, IL, USA*
[i] *Department of Biological Sciences, University of Calgary, Calgary, Alberta, Canada*

ARTICLE INFO

Article history:
Received 4 May 2022
Received in revised form 19 July 2022
Accepted 19 July 2022
Available online 13 September 2022

Keywords:
Anthelmintics
Gastrointestinal nematode
Isotype-1 beta-tubulin
Resistance
RAD-seq
Selection signatures

ABSTRACT

Genome-wide methods offer a powerful approach to detect signatures of drug selection. However, limited availability of suitable reference genomes and the difficulty of obtaining field populations with well-defined, distinct drug treatment histories mean there is little information on the signatures of selection in parasitic nematodes and on how best to detect them. This study addresses these knowledge gaps by using field populations of *Haemonchus contortus* with well-defined benzimidazole treatment histories, leveraging a recently completed chromosomal-scale reference genome assembly. We generated a panel of 49,393 genomic markers to genotype 20 individual adult worms from each of four *H. contortus* populations: two from closed sheep flocks with an approximate 20 year history of frequent benzimidazole treatment, and two populations with a history of little or no treatment. Sampling occurred in the same geographical region to limit genetic differentiation and maximise the detection sensitivity. A clear signature of selection was detected on chromosome I, centred on the isotype-1 β-tubulin gene. Two additional, but weaker, signatures of selection were detected; one near the middle of chromosome I spanning 3.75 Mbp and 259 annotated genes, and one on chromosome II spanning a region of 3.3 Mbp and 206 annotated genes, including the isotype-2 β-tubulin locus. We also assessed how sensitivity was impacted by sequencing depth, worm number, and pooled versus individual worm sequence data. This study provides the first known direct genome-wide evidence for any parasitic nematode, that the isotype-1 β-tubulin gene is quantitatively the single most important benzimidazole resistance locus. It also identified two additional genomic regions that likely contain benzimidazole resistance loci of secondary importance. This study provides an experimental framework to maximise the power of genome-wide approaches to detect signatures of selection driven by anthelmintic drug treatments in field populations of parasitic nematodes.

1. Introduction

Parasitic nematode infections are of major medical and agricultural importance worldwide (Mutombo et al., 2019; Rose Vineer et al., 2020). Control strategies largely depend on the regular use of anthelmintic drugs, which has caused widespread anthelmintic drug resistance in many parasitic nematode species of livestock (Kaplan and Vidyashankar, 2012; Rose Vineer et al., 2020). Addi-

* Corresponding authors.
E-mail address: jsgillea@ucalgary.ca (J.S. Gilleard).

[1] Present address: Wellcome Center for Integrative Parasitology, Institute of Biodiversity Animal Health and Comparative Medicine, College of Medical, Veterinary and Life Sciences, University of Glasgow, Garscube Campus, Glasgow, UK.
[2] Present address: School of Veterinary Medicine, University of Surrey, England, UK.

https://doi.org/10.1016/j.ijpara.2022.07.004
0020-7519/

tionally, concerns are increasing that mass drug administration programmes are selecting for anthelmintic resistance in helminths that infect humans (Krücken et al., 2017; Furtado et al., 2019; Orr et al., 2019; Kotze et al., 2020; Tinkler, 2020). Over the last 30 years, there has been a large amount of research into the molecular genetic basis of anthelmintic resistance, particularly in gastrointestinal nematodes of livestock (Gilleard, 2013). Most of this work has been dominated by candidate gene studies, where certain genes are prioritised based on knowledge of the mode of action of the drug (Kwa et al., 1994; Le Jambre et al., 2000; McCavera et al., 2009; Rufener et al., 2009; Urdaneta-Marquez et al., 2014) or by the extrapolation of genetic studies in the model organism *Caenorhabditis elegans* (Guest et al., 2007; Kaminsky et al., 2008). Although this approach has been successful in some cases, most notably for the benzimidazole (BZ) drug class, it has been much less successful in others (Wit et al., 2021). For example, in the case of the macrocyclic lactones, which is one of the most important broad spectrum classes of anthelmintic drugs, the evidence implicating the leading candidate genes has been inconsistent between studies (Prichard and Roulet, 2007; Glendinning et al., 2011; Janssen et al., 2013; Doyle and Cotton, 2019; Rezansoff et al., 2019).

Genome-wide approaches, which make no a priori assumptions about the underlying mechanisms of resistance, are potentially more powerful approaches to identify anthelmintic resistance loci than candidate gene studies. The most successful helminth example to date was the use of classical linkage mapping to identify a Quantitative Trait Locus (QTL) for oxamniquine (OXA) resistance in the human trematode *Schistosoma mansoni* (Valentim et al., 2013). Subsequent work confirmed the functional importance of a mutation in a sulfotransferase enzyme (SmSULT-OR) gene to the OXA-resistant phenotype (Valentim et al., 2013; Anderson et al., 2018).

The small ruminant parasite *Haemonchus contortus* is the leading parasitic nematode model for anthelmintic resistance research for a variety of reasons, including the availability of well-characterised anthelmintic-resistant isolates, a good understanding of its genetics, and the ability to undertake genetic crosses (Redman et al., 2008, 2012; Hunt et al., 2010; Gilleard, 2013). A chromosomal-scale reference genome assembly and annotation enables genome-wide approaches in this parasitic nematode species (Doyle et al., 2020). This new reference genome was successfully used to map the major ivermectin resistance QTL on chromosome V in two independent laboratory-passaged *H. contortus* strains by two different crossing approaches (Doyle et al., 2019, 2022). However, such genetic crosses are extremely challenging in parasitic nematodes compared with model organisms and have only been demonstrated in a few parasite species (Redman et al., 2012; Laing et al., 2022). An alternative way to map the genetic loci underlying anthelmintic resistance is to use population genomic approaches on field populations. This approach is not only technically simpler and more scalable but is also more likely to identify anthelmintic resistance loci that are relevant to field populations.

As reference genomes for parasitic nematodes continue to improve, and DNA sequencing costs reduce, population genomic studies on natural field populations should become increasingly feasible. However, there is currently a lack of data from field populations with sufficiently well-defined and contrasting drug treatment histories to unambiguously link signals of selection in the genome with specific drug treatments. For example, most *H. contortus* field populations have been subject to treatment with multiple different drug classes and to significant animal movement. Consequently, there is a need for studies on field populations with well-defined drug treatment histories to elucidate the genomic location and nature of signatures of selection associated with specific drug classes.

It is now well established that mutations in the isotype-1 β-tubulin gene are important determinants of BZ resistance in *H. contortus* and other strongylid nematodes (Kwa et al., 1993, 1994, 1995; Beech et al., 1994; Prichard, 2001; Dilks et al., 2020, 2021). However, a key knowledge gap at present is whether the isotype-1 β-tubulin locus is the only major locus under selection by BZ drug treatments or whether there are additional selected loci and, if so, their relative importance (Hahnel et al., 2018). Interestingly, a recent study in which whole-genome sequencing was applied to 233 individual adult *H. contortus* worms from field populations identified multiple regions of the genome that showed signatures of selection including around the isotype-1 β-tubulin locus (Sallé et al., 2019). However, this study could not associate these signatures of selection with treatment by a specific drug class as the populations used had a variety of complex drug treatment histories. A major aim of our current study was to determine which loci in the *H. contortus* genome show strong evidence of selection that are specifically associated with BZ selection in the field.

Another aim of this study was to take advantage of the clear and contrasting BZ drug selection histories of the *H. contortus* populations on government and rural farms in Pakistan to investigate the best technical approach to detect genomic signatures of drug selection in field populations. Reduced-representation sequencing methods, where a random but consistent subset of the genome is sequenced, are potentially powerful and cost-effective for genome-wide methods (Wit and Gilleard, 2017). Larger numbers of organisms and/or samples can be sequenced using this method rather than by whole-genome sequencing at the same cost, and although sequencing costs are dropping, cost is an important consideration when examining larger sample sets, particularly for laboratories outside of the major genome sequencing centres (Andrews et al., 2016; Díaz-Arce and Rodríguez-Ezpeleta, 2019). One of the more widely used reduced-representation approaches is restriction site-associated DNA sequencing (RAD-seq) (Baird et al., 2008; Davey and Blaxter, 2010; Peterson et al., 2012; Fig. 1). This approach has been extremely successful at investigating population diversity and differentiation in a wide range of organisms (Andersen et al., 2012; Kumar and Kocour, 2017; Settepani et al., 2017; Graham et al., 2020). However, it is still a challenge to get a high-density marker set to identify signatures of selection (Hohenlohe et al., 2010; Jacobsen et al., 2014; Wright et al., 2020).

Here, we describe the development of a high density RAD-seq marker set, and its use to investigate the genomic signature(s) of BZ drug selection in *H. contortus* field populations. The strongest signature of BZ drug selection, by far, that was present in two populations with a history of regular BZ treatments, but absent in two untreated populations, was in the genomic region surrounding the isotype-1 β-tubulin gene. Two other genomic regions under drug selection were identified but the signals of selection at these loci were weaker. In addition, we investigated the effect of sample number and read depth, and compared the analysis of individual worm sequence data with pooled sequence data on the ability of RAD-seq to detect genomic selection signatures in order to provide a framework for future experimental design.

2. Materials and methods

2.1. Parasite material

Populations of adult *H. contortus* worms were harvested from four different sheep flocks in the Punjab province of Pakistan (Chaudhry et al., 2016, Fig. 2A). Two populations were sampled from government farm flocks with a history of regular BZ treatment over several decades; Treated 1 (T1) from Okara and Treated

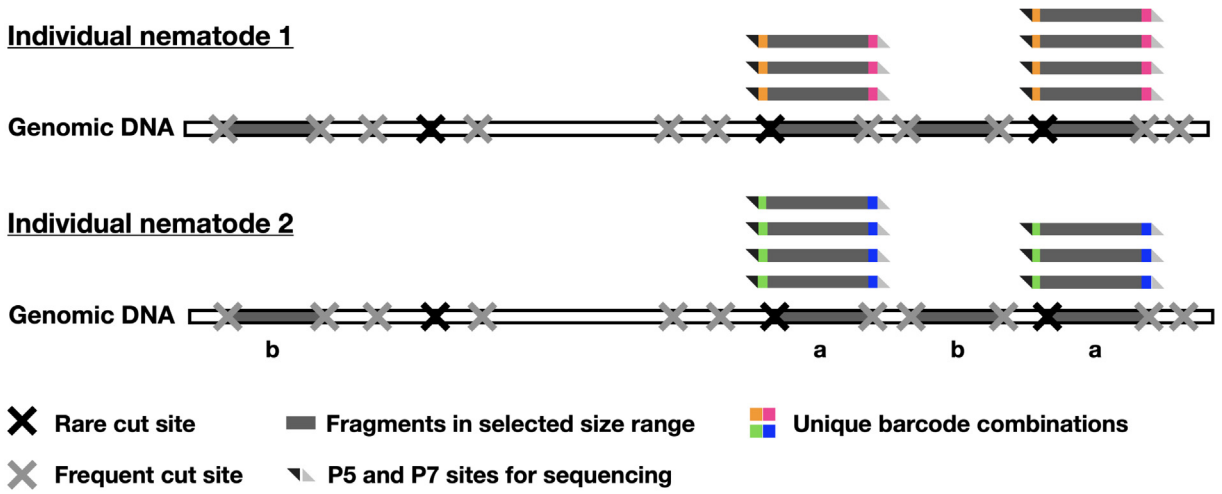

Fig. 1. Schematic overview of double-digest restriction site-associated DNA sequencing (ddRAD-seq), adapted from Peterson et al. (2012). ddRAD-seq is a reduced representation genome sequencing method which aims to sequence a subset of fragments across the genome that is consistent between samples. Before restriction digestion of the genomic DNA, a whole-genome amplification step is used to provide sufficient quantities of DNA for the protocol. The whole-genome amplified DNA from each sample is then individually digested with two restriction enzymes, one which cuts at a recognition site occurring frequently throughout the genome and the other at a recognition site occurring only rarely in the genome. This combination of enzymes determines the number and size distribution of the resulting genomic fragments. After digestion, adapters containing unique barcode combinations are ligated to the double-digested fragments, after which the samples are pooled. A size selection step is then applied to retain only fragments within a preferred size range, limiting the number of fragments that will be sequenced. Fragments of the selected size are indicated as fragments (a) and (b) in the figure. After size selection, two distinct short adapter sequences (Illumina P5 and P7) are incorporated in fragment termini by PCR using primers complementary to the adapter sequences. The P5 and P7 primers anneal to the Illumina flow cell and so this final step ensures that only the originally double-digested fragments are amplified and sequenced on the flow cell. These are indicated as fragments (a) in the figure.

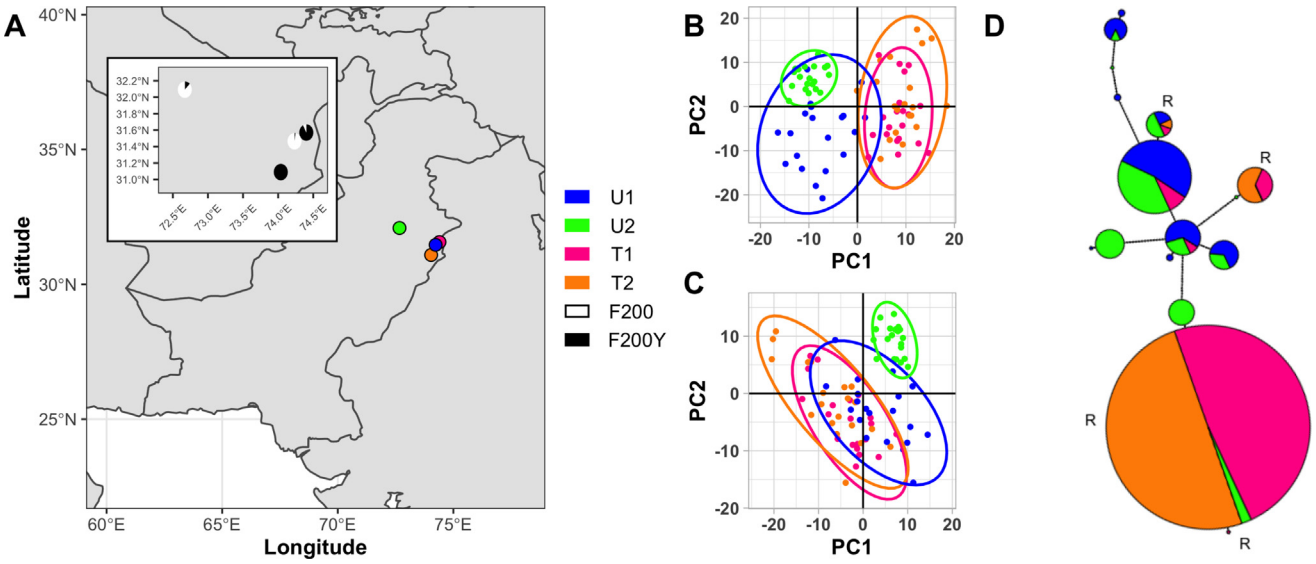

Fig. 2. Overview of sampling locations of four populations of *Haemonchus contortus*, their genetic differentiation and observed levels of resistance conferring isotype-1 β-tubulin alleles. The populations were sampled in four different sheep flocks in the Punjab province of Pakistan (Chaudhry et al., 2016) either from government flocks with a history of regular BZ treatment over several decades (T1 and T2) or from rural flocks (U1 and U2) with little or no history of drug treatment. (A) Sampling locations in the Punjab province of Pakistan; inset shows the percentage of F200Y mutations of the isotype-1 β-tubulin locus. (B) Principle component analysis (PCA) plot comparing single nucleotide polymorphism (SNP) data of the four populations. (C) PCA plot comparing SNP data of the four populations without chromosome I. (D) Haplotype network of amplified sequence variants (ASVs) of the isotype-1 β-tubulin locus amplicon data.

2 (T2) from Jahangirabad (T1 is Pop1S and T2 is Pop3S in Chaudhry et al. (2016)). These government farms established their sheep flocks using local sheep breeds (lohi and kajli) in 1985 and 1989, respectively, and have been alternatively treated with albendazole and oxfendazole, but not other anthelmintic classes, approximately every-three months since their establishment. These herds have been closed to animal movement since they were established. There has been some historical movement of stock between the farms, but no animals have been introduced from elsewhere. Two other populations were sampled from rural flocks with no history of drug treatment, from two abattoirs in the same region; Untreated 1 (U1) and Untreated 2 (U2). Worms were harvested directly from ewe abomasa at necropsy at abattoirs, from sheep carcasses following routine slaughter for human consumption, and stored in 70% ethanol at −80 °C. For this study, 20 females were randomly selected from each sample.

2.2. DNA extraction

Adult female worms were rehydrated in sterile water for 60 min prior to extraction. Tissue was isolated from the anterior portion of the adult worm, avoiding the gonads containing progeny, and DNA was extracted using a protocol adapted from Bennett et al. (2002). After dissection of the animal, the anterior portion was transferred to 600 µl of lysis buffer (384 µl of H_2O, 60 µl of 1 M Tris HCl (pH 8.5), 60 µl of 1% SDS, 60 µL of 0.5 M EDTA (pH 7.5), 12 µl of 5 M NaCl, 12 µl of proteinase K (14–22 mg/mL, Qiagen, USA), and 12 µl of β–mercaptoethanol). Samples were incubated overnight at 55 °C before 2 µl of RnaseA was added (100 mg/ml, Qiagen), and incubated for 15 min at 45 °C. After adding 150 µl of 5 M NaCl and 100 µl of Cetyl Trimethyl Ammonium Bromide (CTAB)/NaCl, samples were incubated at 65 °C for 15 min. An equal volume of phenol:chloroform:isoamyl alcohol (25:24:1, Sigma-Aldrich, Canada) was added and the solution was incubated for 1.5 h on a slow rocker at room temperature (RT). Samples were centrifuged at 3000 *g* for 15 min at 12 °C and the aqueous phase was collected. An equal volume of chloroform:isoamyl alcohol (24:1, Sigma-Aldrich) was added to the aqueous phase and the solution incubated for 1 h at RT, centrifuged as before and the aqueous phase collected. Two volumes of ice-cold ethanol were added and gently mixed. The solution was placed at −20 °C overnight before being centrifuged as before at 4 °C. After removal of the supernatant, the pellet was washed twice with 70% EtOH. After the final wash, the sample was centrifuged at 21,000 *g* for 10 min, the supernatant removed, centrifuged for an additional minute to remove the remainder of the ethanol and the resulting pellet air dried before resuspension in 30 µl of water and incubation overnight at 4 °C. Sample quality was checked by quantification on the Qubit system (ThermoFisher, CA) and A_{260}/A_{280} absorbance ratios on a NanoVue spectrophotometer (Biochrom Spectrophotometers, USA). A portion (2.5 µl) of each sample (46.4–400 ng) was added to a REPLI-g Single Cell Kit (Qiagen) for whole-genome amplification (WGA) following the manufacturer's protocol for amplification of purified genomic DNA.

2.3. Amplicon sequencing of isotype-1 β-tubulin and isotype-2 β-tubulin genes and haplotype network analysis

Amplicon sequencing was used to determine the frequency of single nucleotide polymorphisms (SNPs) in the isotype-1 and isotype-2 β-tubulin genes previously associated with BZ resistance in *H. contortus* – F200Y (TTC > TAC), F167Y (TTC > TAC), E198A (GAA > GCA), or E198L (GAA > TTA) – in each population. The amplicon sequencing protocol and data analysis has been previously described in Avramenko et al. (2015, 2019)) and adapted for isotype-2 β-tubulin with primers shown in Supplementary Table S1. For the haplotype analysis of isotype-1 β-tubulin, reads classified as *H. contortus* by the Mothur (Schloss et al., 2009) pipeline in the amplicon data analysis were extracted from the original FASTQ files. Primers were removed with Cutadapt (Martin, 2011), and haplotype analysis was conducted with DADA2 (Callahan et al., 2016; R Core Team (2013). R: A language and environment for statistical computing. R Foundation for Statistical Computing, Vienna, Austria, https://www.R-project.org/), following their pipeline tutorial for demultiplexed Illumina paired-end reads. Resulting amplicon sequence variants (ASVs) were used to create a haplotype network using ape and pegas in R (Paradis et al., 2004; Paradis, 2010).

2.4. Preparation and sequencing of double-digest single worm RAD libraries

The single-worm WGA samples were readied for library preparation for sequencing following a protocol adapted from Peterson et al. (2012). Post-WGA samples were purified using a standard bead clean-up protocol using AMPure XP beads (Beckman), with 1.5x beads instead of 1.8x sample:bead volume, and eluted in water. The DNA was digested with *Mlu*CI (5 µl of Cut smart buffer, 1.5–2 µg of DNA, 3 µl of *Mlu*CI (New England Biolabs Inc. (NEB, USA), and water to make up to 49 µl) for 3 h at 37 °C after which 3 µl of *Nla*II (NEB) was added and the reaction incubated at 37 °C for a further 3 h. The samples were cleaned as before. Barcoded adapters were ligated in a 50 µl reaction volume, with 4 µl of T4 buffer, 7.5 µl each of adapters P1 and P2, 0.7 µl of T4 ligase (2 M U/ml, NEB), 250 ng of DNA (adapters are shown in Supplementary Table S1) and water. The combination of P1 and P2 adapters was unique to each individual sample. Libraries from individual worms of different populations were randomised to create pools containing 20 individuals each, cleaned as before, and size-selected on a PippinPrep (Sage Science, DMARK Biosciences, Canada) using the standard protocol for Tight Range (190 bp) on a 3% internal standard cartridge, resulting in a fragment range of 190–300 bp with a peak at 210 bp. Quality and fragment size was checked on a Tape Station (Agilent, USA), and P5 and P7 adapters were incorporated per pool by 10 PCR cycles according to the KAPA HiFi Hotstart PCR kit standard protocol (Kapa Biosystems), selectively amplifying fragments with both a *Mlu*CI and a *Nla*II recognition site. The separate samples of 20 pooled individuals each were then combined and cleaned as before. Because the fragments ranged in size, the quantity was checked in triplicate using a Qubit broad range kit, rather than a quantitative PCR approach, and diluted to 4 nM after correction for average size of the sample based on another Tape Station analysis (https://scienceprimer.com/dna-ng-nm-calculator).

The pooled individual worm libraries were sequenced on the Illumina NextSeq platform. Populations U1, U2, T1, and T2 were sequenced on one High Output 2 × 75 bp kit. The U2 population was discarded after only 20.22–53.54% of its reads were mapped to the reference, with the remainder being bacterial contamination. Consequently, the U2 population was re-sequenced using a Mid Output 2 × 75 bp kit. The loading concentration was 1.2 pM, and 50% PhiX was spiked in for diversity due to the low diversity library.

Fragment size selection was based on predicted fragment recovery with the draft genome assembly (GCA_000469685.1 (Laing et al., 2013)) using SimRAD (Lepais and Weir, 2014).

2.5. Quality control and analysis of sequence data

The data were demultiplexed using process_radtags in the Stacks pipeline (Catchen et al., 2013). All samples were assessed for general sequence quality using FastQC (Andrews, S., 2010. FastQC: A Quality Control Tool for High Throughput Sequence Data, https://www.bioinformatics.babraham.ac.uk/projects/fastqc/; Andrews, S., (2015), "FastQC" https://qubeshub.org/resources/fastqc.) before removing adapters using Cutadapt (Martin, 2011). Read quality was high across the full read length for both sequencing runs; therefore, no hard trimming was conducted. Reads were aligned against the chromosomal-scale *H. contortus* reference genome assembly (GCA_000469685.2, *n* = 7 (Doyle et al., 2020)) using Bowtie2 (--local --very-sensitive-local -X 300 -I 80 (Langmead and Salzberg, 2012)). A binary alignment and map (BAM) file was generated for each sample using Samtools by filtering for paired reads only and then sorting (Li et al., 2009). The sorted data was analysed using the programmes gstacks and populations with the –fstats flag from the Stacks pipeline. Only SNPs that were present in three of four populations, in 50% of individuals per population, and at a minimum frequency of 5% were retained in the output. In addition, only the first SNP per RAD locus was

reported to avoid linkage and variable SNP count within a locus to affect the interpretation of the data.

To assess the robustness of the RAD-seq analysis and investigate the limits of its ability to detect signatures of selection, additional analyses were conducted using the same basic parameters but using fewer individual worms per population (5, 10, and 15, randomly selected), as well as fewer reads per individual (1 million (M), 1.5 M, and 2 M reads where possible, randomly selected using seqtk sample). Finally, the raw reads were realigned to an earlier version of the reference genome (GCA_000469685.1, N50 = 0.099 Mb, N50(n) = 876, n = 12,915) (Laing et al., 2013), to illustrate the effect of genome quality on identifying regions of interest in the genome.

2.6. Population differentiation, expected heterozygosity, and linkage disequilibrium analyses to detect signatures of selection

All analyses were performed on data generated by Stacks (version 2.2), reporting one SNP per RAD locus, unless otherwise stated. To examine overall population differentiation, population level F_{ST} values were calculated and a Principal Component Analysis (PCA) was conducted on all reported SNPs across the populations using the vcfR (version 1.8.0) and adegenet (version 2.1.1) packages in R (Jombart and Ahmed, 2011; Knaus and Grünwald, 2017).

To detect regions in the genome where population differentiation was significantly higher than background noise, we used a top candidate method as described in Yeaman et al. (2016). The 99th percentile of all F_{ST} values was determined and F_{ST} values were then binned over 150 kb intervals. Top candidate regions were identified as bins with an exceptional proportion of their total SNPs being F_{ST} outliers based on a binomial distribution. For expected heterozygosity, a similar approach was undertaken. Outliers were defined as expected heterozygosity values falling in the lowest 25th percentile and then binned across 150 kb regions. Top candidate bins were identified as those having a higher than expected proportion of low expected heterozygosity based on a binomial distribution. Linkage disequilibrium per population was calculated in R using the cor() function with "pairwise.complete.obs". These values were binned across 150 kb regions and the percentage of R^2 values above the 99th percentile of all R^2 values per population was recorded.

2.7. Analysis of mock pooled sequence data

All RAD-seq data from individual worms per population were pooled to create mock pooled sequence data. Data were pooled after demultiplexing with process_radtags, as these RAD-specific barcodes would not be present in Illumina sequence data of pooled samples. Samples were then aligned with Bowtie2 as above. The resulting aligned files were subsampled randomly using seqtk, resulting in 100× genome coverage. For analyses of individual samples, average expected heterozygosity was determined for one SNP per RAD locus, therefore bedtools was used to concatenate SNPs within 150 bp of each other to one marker for pooled samples (Quinlan and Hall, 2010; Quinlan, 2014). These subsamples were analysed using PoPoolation Variance-sliding.pl (Variance-sliding.pl --measure pi --min-count 2 --min-qual 20 --min-coverage 15 --max-coverage 400 --pool-size 20 --window-size 1 --step-size 1) and Popoolation2 snp-frequency-diff.pl (snp-frequency-diff.pl --min-count 3 --min-coverage 15 --max-coverage 400 (Kofler et al., 2011a, b), generating Tajima's Pi and F_{ST} statistics.

2.8. Detecting genes in genomic regions under selection

All genes and corresponding proteins within the genomic regions showing consistent signatures of selection in the treated populations across multiple estimates were extracted from the gene annotation file haemonchus_contortus.PRJEB506.WBPS14.annotations.gff3 and the FASTA file haemonchus_contortus.PRJEB506.WBPS14.protein.fa. Potential causal variation in these genes would not necessarily be identified in RAD-data due to limited sequence coverage of the region. Therefore, functional annotation of the selected genes was performed with InterPro version 5.35–74.0 and Pfam database version 32.0 (interproscan.sh -i [input_protein.fa] -d out -dp -t p --goterms -appl Pfam -f tsv).

2.9. Data accessibility

All samples for the ddRAD-seq project are collected under BioProject accession number PRJNA822658. Data and scripts to generate figures are available at https://github.com/ucvm/RAD_Haemonchus/.

3. Results

3.1. Developing a panel of genome-wide RAD-seq markers for H. contortus

Genome-wide RAD-seq markers were generated by digestion of the genome with *Mlu*CI and *Nla*II, fragment size selection of 190–300 bp (peak at 210 bp), and sequencing on an Illumina NextSeq system (2 × 75 bp). On average, 77.7% of the reads mapped to the reference genome sequence (max: 81.4%, min: 60.2%, median: 78.6%). Of the mapped reads, 77.6% passed the paired-read philtre, providing an overall average total of 60.33% of raw reads for further analysis using Stacks (Catchen et al., 2013) (number of reads kept: average = 3,337,301, median = 3,186,605, min = 1,283,698, max = 5,501,942). We kept only those markers present in 50% of individuals per population and in all three populations (75.4% of all primary alignments). Average coverage and marker density for all comparisons are shown in Table 1. With baseline parameters, the range of reads per individual was 4.4X- 14.2X coverage. Marker density across the genome is shown in Supplementary Fig. S1.

3.2. Population-wide genetic diversity and isotype-1 β-tubulin resistance allele frequencies

Genome-wide pairwise F_{ST} was low between all populations, based on population differentiation across 43,587–48,227 markers (Table 2). Population differentiation was highest in the pairwise comparisons involving population U2 (Table 2). PCA illustrated the genetic similarity of the two drug-treated populations (T1 and T2), with some overlap with U1 but not U2, consistent with the F_{ST} results (Fig. 2B). Removing variation on chromosome I (which contains the isotype-1 β-tubulin gene) decreases differentiation between U1 and T1 and T2 (Fig. 2C). Although U2 was collected in the Punjab province, it was collected in Sargodha, about 200 km from Lahore, where the other populations were collected. This distance potentially explains the slightly increased levels of differentiation between U2 and the other populations (Fig. 2A).

Of the isotype-1 β-tubulin SNPs previously associated with BZ resistance in *H. contortus*, only 200Y (TTC > TAC) was detected in the populations after genotyping by amplicon sequencing. The frequencies of F200Y in the U1, U2, T1, and T2 populations were 2.5%, 12.5%, 100%, and 92.5%, respectively, consistent with their drug treatment history and indicative of their BZ resistance status (Fig. 2A inset). The most common resistance isotype-1 β-tubulin

Table 1
Overview of coverage and average marker recovery across the *Haemonchus contortus* genome using different analysis parameters and data subsets.

Dataset	Average coverage per marker	Marker count
Mapping to reference genome: GCA_000469685.2		
Baseline *(50% individuals, 3 populations)*	9.1	49,393
Stringent *(75% individuals, 3 populations)*	9.1	26,269
Mapping to reference genome: GCA_000469685.1		
Baseline *(50% individuals, 3 populations)*	9.8	42,987
Data Subsets *(50% individuals, 3 populations)*		
Population size = 15	9.0	45,226
Population size = 10	9.4	49,687
Population size = 5	9.0	52,532
Read depth = 2.0 M/sample	7.4	42,818
Read depth = 1.5 M/sample	6.3	37,432
Read depth = 1.0 M/sample	5.0	30,136
Read depth = 0.5 M/sample	3.3	18,283
Read depth = 0.25 M/sample	2.3	7,769

haplotypes are present at high frequency in both T1 and T2 populations (Fig. 2D). The isotype-2 β-tubulin gene was also genotyped by amplicon sequencing for all individual worms to identify potential candidate resistance mutations at codons 167, 198, and 200. All worms were homozygous for "susceptible alleles" (198E, and 200F), except for one worm in population U1, which was heterozygous for a F200Y (TTC > TAC) allele.

3.3. The major region of genetic differentiation between treated and non-treated populations centres around the isotype-1 β-tubulin locus on chromosome I

All four pairwise genome-wide comparisons between the two treated and two untreated populations showed a major region of elevated F_{ST} on chromosome I, centred around the isotype-1 β-tubulin locus (chromosome I, around 7.0 Mb, Fig. 3A). This region depended on the particular pairwise comparison but was between 3.5 and 10 Mb across all comparisons. Pairwise comparisons between either the two treated or untreated populations did not have an elevated F_{ST} in this region (Fig. 3A). In addition, a weaker region of elevated F_{ST} in a region of chromosome 2, which included the isotype-2 β-tubulin locus, was identified for the T2-U1 and T2-U2 but not the T1-U1 and T1-U2 pairwise comparisons.

3.4. Patterns of expected heterozygosity and linkage disequilibrium indicate a strong signature of selection around the isotype-1 β-tubulin locus and identify a second locus under selection on chromosome I

In the treated but not the untreated populations, the region surrounding the isotype-1 β-tubulin gene, which is located on chromosome I (7.027.492–7.031.447), has distinctly reduced expected heterozygosity (position range 5,708,200–8,113,930) and elevated linkage disequilibrium (position range 6,075,000–8,325,000) (Fig. 3B and 4). There is a second region on chromosome 1 with a distinct decrease in expected heterozygosity (position range 26,568,594–26,676,298) and an elevated linkage disequilibrium (position range 26,025,000–26,625,000) (Fig. 4). A third region on chromosome 2 has a region of reduced expected heterozygosity in treated population T2 (position range 13,221,871–13,270,135), close to the isotype-2 β-tubulin gene (13.433.191–13.438.615) (Fig. 3B). Linkage disequilibrium around the third region is not elevated (Supplementary Fig. S2).

Table 2
Pairwise F_{ST} values between populations of *Haemonchus contortus* sampled in four different sheep flocks in the Punjab province of Pakistan (Chaudhry et al., 2016). Two populations, Treated 1 (T1) and Treated 2 (T2), were sampled from government farm flocks with a history of regular BZ treatment over several decades. Untreated 1 (U1) and Untreated 2 (U2) were sampled from rural flocks with little or no history of drug treatment.

Population	T1	T2	U1	U2
T1		0.023	0.031	0.047
T2			0.033	0.046
U1				0.037

3.5. Gene models within the regions defined by the signals of selection in populations T1 and T2

With the chromosomal-scale reference genome, the RAD-seq data were used to detect three genomic regions with signatures of selection shared by the treated populations. With the gene annotations that accompany this genome, we further explored these regions for genes related to BZ resistance. The genomic ranges for the regions under selection were based on population diversity, reduced heterozygosity, and linkage disequilibrium analyses and are as follows: 1) chromosome I: 5.7–9.6 Mb; (2) chromosome I: 22.95–26.7 Mb; and (3) chromosome II: 12.45–15.75 Mb. These regions were based on the widest ranges across all estimates, except for region 1, which was narrowed based on expected heterozygosity and linkage disequilibrium. Region 2 based on F_{ST} estimates ranged from 22.95-23.85 Mb, and for expected heterozygosity and linkage disequilibrium from 25.95-26.7 Mb. For completeness we included all genes from 22.95-26.7 Mb in the Supplementary Table S2. In total, region 1 contains 353 genes, region 2 contains 259 genes and region 3 contains 206 genes (Supplementary Table S2). As discussed, region 1 contains isotype-1 β-tubulin (HCON_00005260), and region 3 contains contains isotype-2 β-tubulin (HCON_00043670).

3.6. Effect of sequencing depth, sample size, population structure, and genome assembly quality on the signature of selection detected by F_{ST}

We investigated the amount of RAD-seq data required to detect the signature of selection, as measured by the elevation in F_{ST} by randomly sub-sampling the dataset. As expected, decreasing the numbers of individuals per population in the analysis decreases the signal of elevated F_{ST} around the isotype-1 β-tubulin gene. However, the signal remains detectable even when data from as few as five individual worms were included in the analysis, especially for the comparisons between the treated populations (T1 and T2) and the U1 untreated population (Fig. 5A, Supplementary Fig. S3). Decreasing the number of reads per individual only minimally affected the elevation of F_{ST} around the isotype-1 β-tubulin locus until the coverage drops below 3.3X (read depth 0.5 M), particularly in comparisons with the more genetically divergent U2 population (Table 1, Fig. 5B, Supplementary Fig. S4).

3.7. Ability to detect signatures of selection using pooled sequence analysis

We compared the ability of a pool-seq approach to detect the signature of selection with that of the single worm approach by pooling the individual worm RAD-seq data for each population. Using Popoolation2, 32,234 SNPs were identified as differential in at least one pairwise population comparison (Fig. 6C, Supplementary Fig. S5, (Kofler et al., 2011a)). These pairwise comparisons show a peak in F_{ST} around the isotype-1 β-tubulin gene, especially for comparisons between both treated populations and U1, with a less clear peak in the comparison with U2. Diversity (π) was deter-

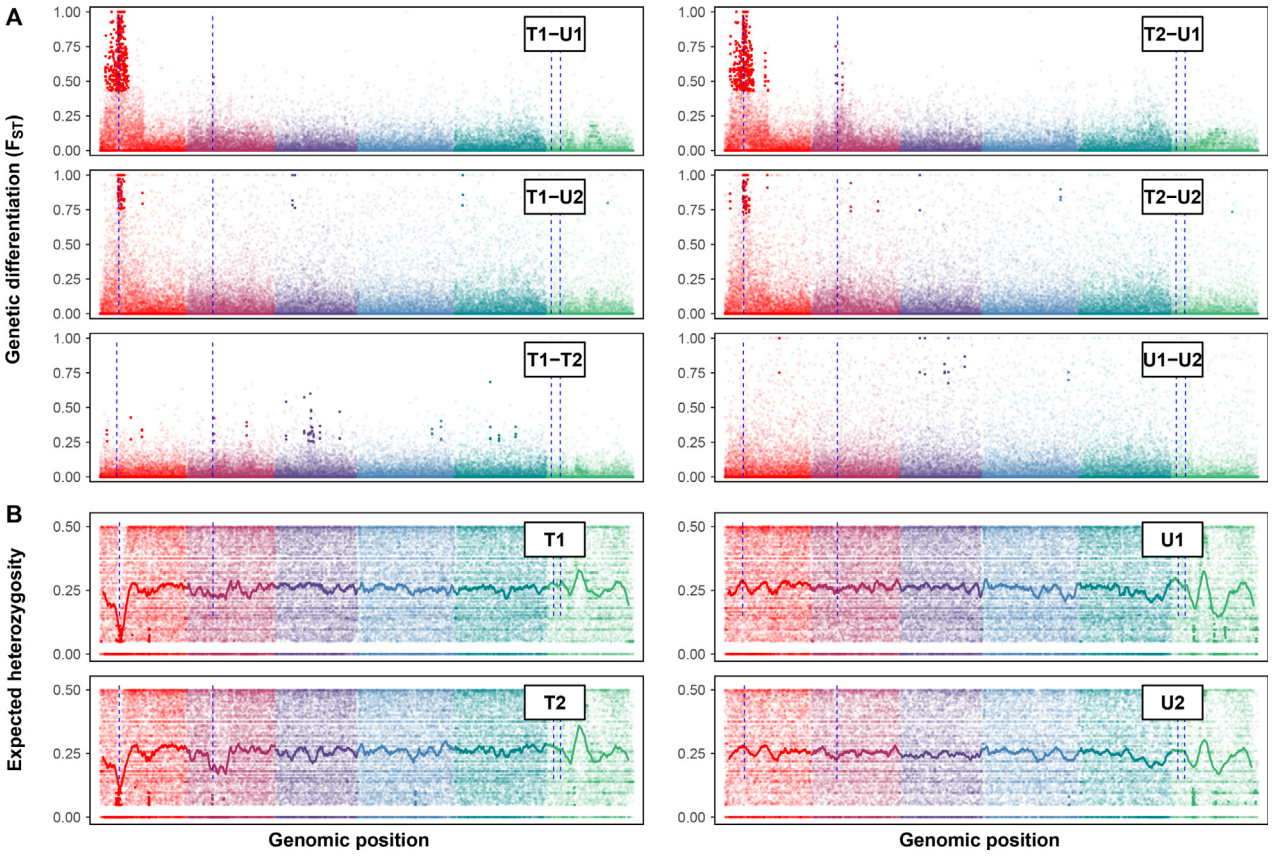

Fig. 3. Genome-wide genetic differentiation and levels of nucleotide diversity across the genome of *Haemonchus contortus*. (A) Genome-wide pairwise F_{ST}. (B) Genome-wide expected heterozygosity estimates per population. Chromosomes are indicated by different colours and ordered from I to V with X on the far right in green. Bolded data points represent loci with an F_{ST} significantly different from background noise, as described by the top candidate test (Yeaman et al., 2016) and in Section 2. The blue lines indicate the locations of isotype-1 β-tubulin on chromosome I, isotype-2 β-tubulin on chromosome II, and isotype-3 and 4 β-tubulin on chromosome X. The solid line in B is the rolling average across 500 genomic loci. T, treated group; U, untreated group.

mined with all available SNP data, with 27,719–113,917 estimates across the genome. These loci were then analysed with Popoolation using the loci as a gene map, with 5,764–14,156 π estimates per population. None of the regions under selection as detected with individual samples were identified with diversity estimates in the pooled analysis (Supplementary Fig. S6).

4. Discussion

The small ruminant gastrointestinal parasite *H. contortus* is the leading parasitic nematode model used for anthelmintic resistance research (Gilleard, 2013; Wit et al., 2021). The primary aim of this study was to investigate the number, genomic location(s), and characteristics of the signatures of selection specifically associated with long-term routine use of BZ drugs in *H. contortus* in the field. The widespread use of anthelmintic drugs in livestock, together with high parasite migration as a result of animal movement, makes it difficult to find *H. contortus* populations that have either been subject to selection with a single drug class or have not been exposed to drug selection at all. However, our previous work identified two *H. contortus* populations from government farms in Pakistan (designated T1 and T2 in this paper) that have been subjected to intensive selection pressure by BZs over many years but not to selection by other drug classes (Chaudhry et al., 2016). In the present work we have compared these with two *H. contortus* populations from rural sheep flocks from the same region (designated U1 and U2 in this paper) that are likely to have had minimal exposure to drug selection (Chaudhry et al., 2016). Amplicon sequencing confirmed a high frequency of the previously known F200Y isotype-1 β-tubulin BZ resistance mutation in the two selected populations (T1 and T2) and a very low frequency in the two unselected populations (U1 and U2), consistent with the respective drug selection histories of the populations (Fig. 2A). Genome-wide pairwise F_{ST} analysis of 43,587–48,227 RAD-seq markers confirmed low levels of genetic differentiation between the four populations with U2 being the most differentiated. Consequently, these populations were particularly suitable to investigate the number, genomic location(s) and characteristics of the signatures of selection specifically associated with long-term routine use of BZ drugs in the field. In this paper, we have presented a reduced representation genome-wide approach, in which a large panel of RAD-seq markers was mapped to the recently completed *H. contortus* chromosomal-scale genome assembly, to identify the main genetic loci under selection by long term use of BZs in these *H. contortus* field populations (Doyle et al., 2020). A single-worm genotyping approach was chosen, together with study populations from the same geographical region and minimal genetic differentiation, to maximise sensitivity for detecting signatures of selection in parasite field populations. This experimental design also allowed us to sub-sample in different ways and pool our data in order to investigate how the sensitivity of signal detection varied in terms of sample number and read depth.

4.1. The major genomic signature of selection associated with BZ selection in two H. contortus field populations surrounds the isotype-1 β-tubulin locus

There is a substantive body of work demonstrating the importance of a number of non-synonymous mutations in the isotype-

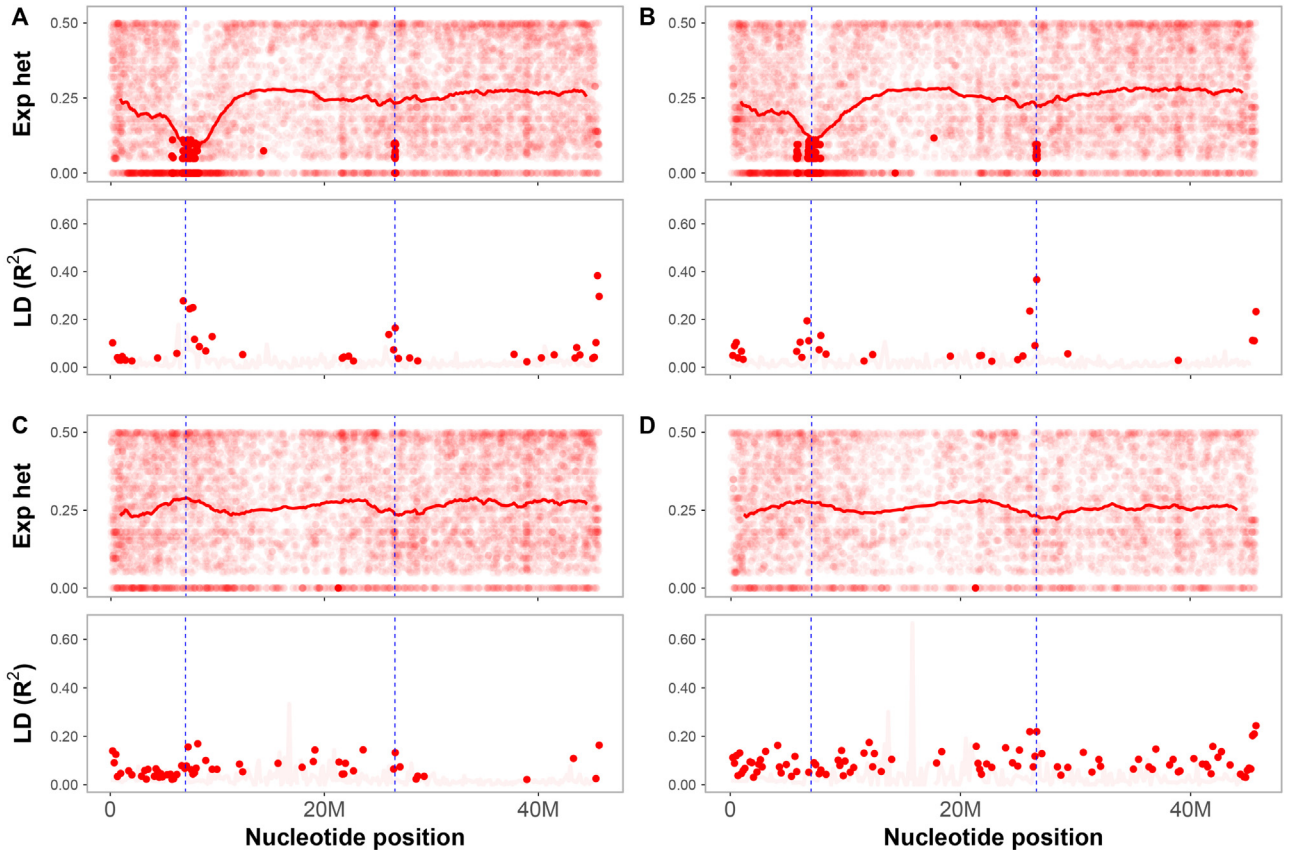

Fig. 4. Chromosome I expected heterozygosity (Exp het), and linkage disequilibrium (LD; R^2). (A) Population T1; (B) population T2 (C) population U1, and (D) population U2. Bolded data points represent loci significantly different from background noise, as described by the top candidate test (Yeaman et al., 2016) and in Section 2. Opaque points and lines indicate non-significant loci. The two dashed lines indicate isotype-1 β-tubulin (left, 7.027.492–7.031.447) and the second locus on chromosome I (right, approximately 26,596,797 Mb). The solid line in expected heterozygosity plots is the rolling average across 500 genomic loci.

1 β-tubulin gene in BZ resistance in *H. contortus* and related ruminant gastrointestinal nematodes of the superfamily trichostrongyloidea (Gilleard, 2006; reviewed in Kotze et al., 2020). This work includes studies that show evidence of selection and high frequencies of codon F167Y, E198A, E198L, and F200Y mutations in BZ-resistant parasite populations, and a recent CRISPR-Cas9 genetic study that showed that these specific substitutions in the *C. elegans ben-1* β-tubulin gene are sufficient to confer BZ resistance without a fitness cost (Dilks et al., 2020). There is also evidence to suggest that, although these isotype-1 β-tubulin gene mutations are important determinants of BZ resistance, other loci may also play a role. For example, in *H. contortus,* deletion of the isotype-2 β-tubulin gene (Kwa et al., 1993; Doyle et al., 2022) and increased levels of BZ glycosidation due to increased UDP-glucuronosyltransferase (UGT) expression (Matoušková et al., 2018) have been suggested to contribute to resistance. In addition, in *C. elegans,* a QTL on chromosome IV that does not map to the *ben-1* locus, has been shown to underlie the BZ resistance phenotype of some field populations (Zamanian et al., 2018), as well as a QTL on the X chromosome (Hahnel et al., 2018). Whole-genome-sequencing of adult *H. contortus* worms from different regions of the world confirms historical selection around the isotype-1 β-tubulin locus in addition to many other loci with signatures of selection (Sallé et al., 2019). Consequently, although isotype-1 β-tubulin gene mutations are clearly important causes of BZ resistance in *H. contortus,* their relative importance with respect to other genetic loci remains a major knowledge gap.

The genome-wide data presented here revealed that the dominant signal of selection for the two different BZ-selected *H. contortus* field populations (T1 and T2) was centred on the isotype-1 β-tubulin locus on the left arm of chromosome I. No such signal was present in the two populations with a history of little or no BZ selection (U1 and U2). The selection signal is clearly defined by a region of elevated F_{ST} in pairwise comparisons of the two treated with the two non-treated populations and by reduced expected heterozygosity and elevated linkage disequilibrium in the selected but not the unselected populations. The region of elevated F_{ST} extends across a broad region of the left arm of chromosome I (1,663,419–11,549,932) but the regions of reduced nucleotide diversity and elevated linkage disequilibrium are much narrower (expected heterozygosity: 5,708,200–8,113,930; LD: 6,450,000–8,325,000). The isotype-1 β-tubulin gene is located centrally in these regions (7,027,492–7,031,447). Overall, these results strongly suggest that the isotype-1 β-tubulin gene is the single most important BZ resistance locus in the *H. contortus* genome of field populations on both government farms examined in this study.

The T1 and T2 *H. contortus* populations may not be completely independent because the flocks were founded by animals from the same region 30 years ago and there may have been some historical animal movement between the farms during the intervening period (Chaudhry et al., 2016). Interestingly, the same major isotype-1 β-tubulin resistance haplotypes were detected by short-read amplicon sequencing (Fig. 2D). Also, pairwise F_{ST} values of the RAD-seq markers surrounding isotype-1 β-tubulin locus were not elevated in pairwise comparisons between the T1 and T2 populations. Together, these suggest the same resistance alleles are present in the two populations and so could have common ori-

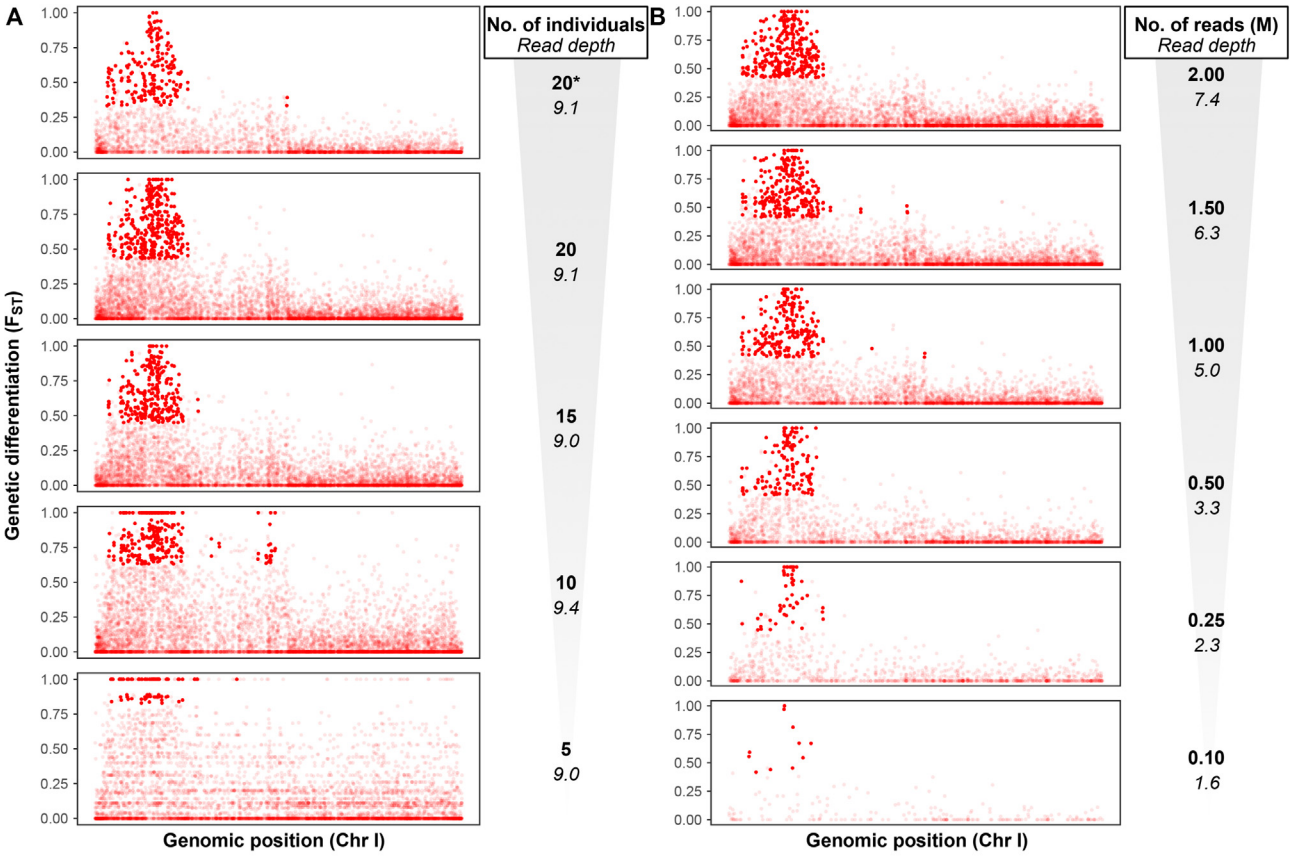

Fig. 5. F_{ST} analysis between two *Haemonchus contortus* populations: treated population 1 (T1) and untreated population 1 (U1). Each dot represents a genomic locus and solid colours represent loci with an F_{ST} significantly above background noise, as described by the top candidate method (Yeaman et al., 2016). (A) F_{ST} estimates across chromosome I with decreasing numbers of individuals per population. 20*: stringent, variants are called when represented in 75% of individuals per population. 20, 15, 10 and 5: variant data present for 50% of the individuals per population, 20-15-10-5. (B) F_{ST} estimates across chromosome I for decreasing numbers of reads per individual sample. Variant data had to be present in 50% of the individuals per population, but only the indicated number of reads was used per sample. Read depth indicated under read count.

gins. Nevertheless, these two populations have been independently selected by BZ treatment for around 30 years and our data reveal the region surrounding the isotype-1 β-tubulin locus is the most strongly selected in both cases.

4.2. Additional genomic regions show signatures of selection after BZ treatments

In addition to the predominant selection signature surrounding the isotype-1 β-tubulin locus in both the T1 and T2 populations, the RAD-seq genome-wide scans detected at least one other region of interest towards the middle of chromosome I (22.95–26.7 Mb). This region had a clear signature of selection – as defined by increased population differentiation, reduction in nucleotide diversity and elevated linkage disequilibrium – in the T1 and T2 but not the U1 and U2 populations (Figs. 3 and 4A,B). The region encompasses 259 genes. A third region of potential interest was identified on chromosome II (Fig. 3; region: 12.45–15.75 Mb) encompassing 206 genes, which was marked by elevated F_{ST} between both the treated T1 and T2 isolates and U1 but not U2 (Fig. 3A). Additionally, this region has reduced nucleotide diversity in T2 but not the other populations (Fig. 3B). The resolutions of the approaches used here are not suitable to define the precise genomic coordinates of the limits of the regions of the genomic signature of selection or to identify the individual relevant genes within the regions. Consequently, we have not speculated on which individual genes might harbour causal resistance mutations but have listed the genes in these regions in Supplementary Table S2 for reference purposes.

It is interesting to note that the region on chromosome 2 includes the isotype-2 β-tubulin (13.433.191–13.438.615). However, short-read amplicon sequencing of a region encompassing codons 167, 198 and 200 of the isotype-2 β -tubulin gene in the T1 and T2 populations did not detect F167Y, E198A, E198L or F200Y candidate resistance mutations in this gene. The potential role of the isotype-2 β-tubulin gene with regards to BZ resistance in these populations remains unclear.

4.3. Double-digest RAD-seq marker panel development for genome-wide analysis

In this work we explored the utility of a reduced-representation genotyping approach, double-digest RAD-seq (ddRAD-seq), for detecting signatures of drug selection in a parasitic nematode genome due to its potential cost effectiveness in large-scale field studies, even for laboratories with relatively limited budgets. The challenges and opportunities of RAD-seq to detect loci associated with adaptation have recently been discussed extensively (Catchen et al., 2017; Lowry et al., 2017a,b; McKinney et al., 2017). The extent of linkage disequilibrium (LD), the availability of a reference genome, and the marker density needed for detection of adaptation are the main challenges to address. For this study, we generated ddRAD-seq data from 20 individual worms from each of four populations, following whole-genome amplification.

To date, most published applications of ddRAD-seq on metazoan organisms have involved relatively small marker panels (up

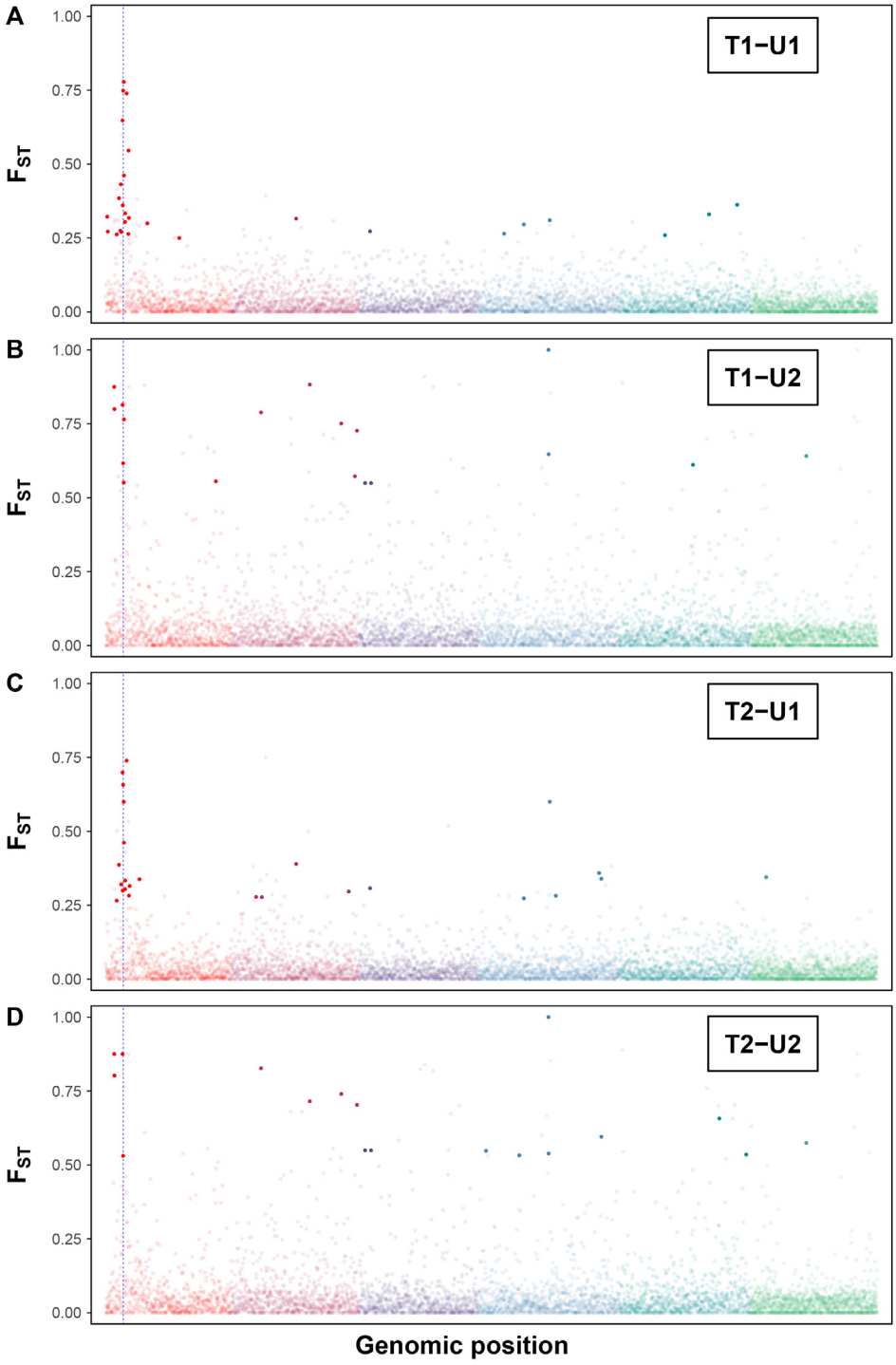

Fig. 6. Pairwise F_{ST} analysis between pooled treated (T) and untreated (U) field populations of *Haemonchus contortus*. Each dot represents a variable locus between the paired populations; solid colours represent loci with a F_{ST} estimate, as described by the top candidate method (Yeaman et al., 2016). The dashed blue line indicates the position of isotype-1 β-tubulin.

to one marker per ~20.9 kb according to a recent review of SNP recovery in aquaculture species (Houston et al., 2020)) and have successfully been used to study population structure. With regard to genome-wide scans to look for signatures of selection, a major challenge is to develop sufficiently dense marker panels across the genome. For most non-model organisms the extent of LD is unknown, complicating the prediction of the number of markers needed to detect signatures of selection. Another challenge is allelic dropout, which occurs as a result of restriction site heterogeneity, and limits the number of recovered loci that are shared between populations (Davey et al., 2013; Puritz et al., 2014). For *H. contortus*, allelic dropout is likely due to its extremely high levels of genetic diversity (reviewed in Gilleard and Redman (2016)). We performed an in silico digestion with the previously published draft reference genome (Laing et al., 2013; GCA_000469685.1) to choose a combination of restriction enzymes and fragment sizes to produce a panel of ~50 k markers that we could recover from at least three of the four populations. At an average of one marker

per 6 kb, this panel represents one of the densest ddRAD-seq marker sets produced for a metazoan organism to date. Two recent papers have described RAD-seq SNP marker panels for *H. contortus* with 2667 (Luo et al., 2017) and 82,271 (Khan et al., 2019) markers, respectively. Although the latter study reported a large number of SNPs, this is not comparable to the present study because they reported multiple SNPs per RAD-seq marker and genotyped pooled genomic DNA to study genetic diversity within and between five populations from different countries.

4.4. Considerations to optimise genome-wide approaches to identify signatures of selection in parasitic nematode field populations

Our study and methodology were designed to maximise the sensitivity of detection of the genomic signals of selection associated with BZ treatments of *H. contortus* in the field. The single worm ddRAD-seq dataset that we generated comprised an average sequence depth of greater than nine reads per marker per sample that we examined in a number of ways to investigate how the sensitivity of detection, based on pairwise F_{ST} analysis and expected heterozygosity, was impacted by the number of individuals, total read depth and reference genome quality. We also investigated the ability of pooled sequence data to detect the signals.

Haemonchus contortus has substantial population structure between countries and a low but discernible population structure within countries (reviewed by Gilleard and Redman, 2016). The identification of genomic signatures of selection in specific regions of the genome can be confounded by population structure (Andolfatto, 2001). Consequently, the four study populations were taken from the same geographical region to limit the extent of between-population genetic differentiation across the genome. The expected limited differentiation was confirmed by the genome-wide F_{ST} values of less than 0.05 for all pairwise comparisons (Table 2). Further, most of the genetic differentiation between the populations was accounted for by chromosome I, suggesting that it was mainly the result of selection at the isotype-1 β-tubulin locus (Fig. 2B,C). Population U2 appeared to be the most genetically distinct of the four populations if the variation on chromosome I is ignored (Fig. 2C). There are two alternative explanations for this: (i) genuine genetic differentiation of this population with respect to the others, especially given the relative distance of the sampling location of U2 in Sargodha compared with those of T1, T2 and U1 in Lahore (all four located in the Lahore region), or (ii) a technical artifact as a result of generating the RAD-seq data for this population on a separate sequencing run as a result of initial poor read recovery of that sample. Fragment size selection during library preparation could have affected the recovered markers. However, based on the markers shared across all populations, this is not a significant concern. Whatever the cause, the strength of the signature of selection around the isotype-1 β-tubulin locus was much lower in pairwise F_{ST} comparisons using the U2 than the U1 population (Fig. 3). This illustrates the importance of careful matching of parasite populations being compared, and control of experimental procedures, to minimise genome-wide differentiation and so maximise the sensitivity of detection.

The signature of selection around isotype-1 β-tubulin could be detected with RAD-seq data from as few as five individual worms per population and as little as two reads per marker when 20 individuals were used (Table 1 and Fig. 5). Based on the data presented here, aiming for a 5–6.5× coverage of 1.1–1.4% of the genome after data cleaning should allow detection of strong signatures of selection. The number of markers expected based on the species of interest and enzyme combination can be calculated in silico (Lepais and Weir, 2014). For expected heterozygosity, the signatures of selection disappear earlier than for F_{ST}; at less than 15 individuals and between 1 and 0.5 M reads (Supplementary Figs. S7 and S8). An advantage of expected heterozygosity is that populations do not have to be as carefully matched.

Draft reference genome sequences are becoming available for an increasing number of parasitic nematode genomes (50 Helminth Genomes Project, 50 HGP; https://www.sanger.ac.uk/science/collaboration/50hgp). However, there are still very few chromosomal-scale reference genome assemblies for these organisms (but see Doyle et al., 2020). Consequently, genome-wide analyses in parasitic nematodes are generally undertaken using draft reference genomes with limited contiguity (Hunt et al., 2016; Choi et al., 2017; Łopieńska-Biernat et al., 2019). In order to simulate this situation, we mapped the full set of RAD-seq read data against a previously published *H. contortus* draft reference genome ((Laing et al., 2013), GCA_000469685.1). Numerous scaffolds with elevated F_{ST} relative to the rest of the genome were identified as showing a signal of selection (Supplementary Fig. S9). In the absence of positional information for the different genomic scaffolds, this data could be potentially misinterpreted as evidence of multiple signatures of selection being present in the genome when in fact it is due to the hitchhiking effect of a single large selective sweep around the isotype-1 β-tubulin locus. This is an important point to consider when working with draft reference genomes that still have relatively poor contiguity.

We also compared the detection of genomic selection signatures using pooled versus single-worm RAD-seq data. We pooled data from individual samples by merging reads from all samples per population into one sample and selecting enough reads for 100× coverage. F_{ST} is high around the isotype-1 β-tubulin gene in comparisons with U1, but it is not significant in comparisons with U2 (Supplementary Fig. S5). This result indicates the limited power of F_{ST} estimates in pooled populations if there is some population structure present. For expected heterozygosity no evidence of selective sweeps was detected using the pooled data (Supplementary Fig. S6). The use of pooled data for genome-wide scans can be improved by increasing sample counts (Lynch et al., 2014) but clearly the ability to do this will depend on the number of well-defined isolates and the budget available. Our data provides a framework to balance the relative merits of sequencing a smaller number of worms at low depth from a small number of populations compared with undertaking Poolseq using greater sequencing depth on a greater number of populations.

In summary, this study illustrates the power of genome-wide approaches to identify signatures of selection associated with long-term anthelmintic treatment of parasitic nematodes in the field. It has shown the critical importance of minimising the population structure when selected and unselected populations are being compared, and the greater sensitivity achieved by single-worm sequencing compared with Poolseq approaches. We have shown that the isotype-1 β-tubulin gene is quantitatively by far the most important BZ resistance locus in the *H. contortus* genome in the two field populations subjected to long-term drug treatment. Interestingly however, we have identified two additional loci that likely harbour mutations associated with BZ resistance but are quantitatively of lesser importance than isotype-1 β-tubulin. Further investigation of these regions may reveal new genes associated with BZ resistance.

Acknowledgements

We would like to thank Dr. Russell Avramenko, Dr. Stephen Doyle, Dr. Axel Martinelli, and the members of the HPI training program for their support during various aspects of the project. We would also like to thank WormBase ParasSite for hosting the *H. contortus* genome and annotation. This research was funded or in part by the Natural Sciences and Engineering Research Council of Canada (grant number 2015-03976, to J.S.G); Results Driven

Agriculture Research, Canada (grant number 2019F022R, to J.S.G.), the Wellcome Trust, UK (grant number 206194); and National Institutes of Health, USA (grant number 5R01AI153088 to E.C.A and J.S.G.). For the purpose of Open Access, the author has applied a CC BY public copyright license to any Author Accepted Manuscript version arising from this submission.

Appendix A. Supplementary data

Supplementary data to this article can be found online at https://doi.org/10.1016/j.ijpara.2022.07.004.

References

Andersen, E.C., Gerke, J.P., Shapiro, J.A., Crissman, J.R., Ghosh, R., Bloom, J.S., Félix, M.-A., Kruglyak, L., 2012. Chromosome-scale selective sweeps shape *Caenorhabditis elegans* genomic diversity. Nat. Genet. 44 (3), 285–290.

Anderson, T.J.C., LoVerde, P.T., Le Clec'h, W., Chevalier, F.D., 2018. Genetic crosses and linkage mapping in schistosome parasites. Trends Parasitol. 34 (11), 982–996.

Andolfatto, P., 2001. Adaptive hitchhiking effects on genome variability. Curr. Opin. Genet. Dev. 11 (6), 635–641.

Andrews, K.R., Good, J.M., Miller, M.R., Luikart, G., Hohenlohe, P.A., 2016. Harnessing the power of RAD-seq for ecological and evolutionary genomics. Nat. Rev. Genet. 17 (2), 81–92.

Avramenko, R.W., Redman, E.M., Lewis, R., Yazwinski, T.A., Wasmuth, J.D., Gilleard, J. S., Serrano Ferron, E., 2015. Exploring the gastrointestinal "nemabiome": deep amplicon sequencing to quantify the species composition of parasitic nematode communities. PLoS One 10, (12) e0143559.

Avramenko, R.W., Redman, E.M., Melville, L., Bartley, Y., Wit, J., Queiroz, C., Bartley, D.J., Gilleard, J.S., 2019. Deep amplicon sequencing as a powerful new tool to screen for sequence polymorphisms associated with anthelmintic resistance in parasitic nematode populations. Int. J. Parasitol. 49 (1), 13–26.

Baird, N.A., Etter, P.D., Atwood, T.S., Currey, M.C., Shiver, A.L., Lewis, Z.A., Selker, E.U., Cresko, W.A., Johnson, E.A., Fay, J.C., 2008. Rapid SNP discovery and genetic mapping using sequenced RAD markers. PLoS One 3, (10) e3376.

Beech, R.N., Prichard, R.K., Scott, M.E., 1994. Genetic variability of the beta-tubulin genes in benzimidazole-susceptible and -resistant strains of *Haemonchus contortus*. Genetics 138, 103–110.

Bennett, A.B., Anderson, T.J.C., Barker, G.C., Michael, E., Bundy, D.A.P., 2002. Sequence variation in the *Trichuris trichiura* β-tubulin locus: implications for the development of benzimidazole resistance. Int. J. Parasitol. 32 (12), 1519–1528.

Callahan, B.J., McMurdie, P.J., Rosen, M.J., Han, A.W., Johnson, A.J.A., Holmes, S.P., 2016. DADA2: High-resolution sample inference from Illumina amplicon data. Nat. Methods 13 (7), 581–583.

Catchen, J., Hohenlohe, P.A., Bassham, S., Amores, A., Cresko, W.A., 2013. Stacks: an analysis tool set for population genomics. Mol. Ecol. 22 (11), 3124–3140.

Catchen, J.M., Hohenlohe, P.A., Bernatchez, L., Funk, W.C., Andrews, K.R., Allendorf, F. W., 2017. Unbroken: RAD-seq remains a powerful tool for understanding the genetics of adaptation in natural populations. Mol. Ecol. Resour. 17 (3), 362–365.

Chaudhry, U., Redman, E.M., Ashraf, K., Shabbir, M.Z., Rashid, M.I., Ashraf, S., Gilleard, J.S., 2016. Microsatellite marker analysis of *Haemonchus contortus* populations from Pakistan suggests that frequent benzimidazole drug treatment does not result in a reduction of overall genetic diversity. Parasit. Vectors 9, 349.

Choi, Y.-J., Bisset, S.A., Doyle, S.R., Hallsworth-Pepin, K., Martin, J., Grant, W.N., Mitreva, M., Andersen, E.C., 2017. Genomic introgression mapping of field-derived multiple-anthelmintic resistance in *Teladorsagia circumcincta*. PLoS Genet. 13, (6) e1006857.

Davey, J.W., Blaxter, M.L., 2010. RAD-seq: next-generation population genetics. Brief. Funct. Genomics 9 (5-6), 416–423.

Davey, J.W., Cezard, T., Fuentes-Utrilla, P., Eland, C., Gharbi, K., Blaxter, M.L., 2013. Special features of RAD Sequencing data: implications for genotyping. Mol. Ecol. 22, 3151–3164.

Díaz-Arce, N., Rodríguez-Ezpeleta, N., 2019. Selecting RAD-Seq data analysis parameters for population genetics: the more the better? Front. Genet. 10, 533.

Dilks, C.M., Koury, E.J., Buchanan, C.M., Andersen, E.C., 2021. Newly identified parasitic nematode beta-tubulin alleles confer resistance to benzimidazoles. bioRxiv. https://doi.org/10.1101/2021.07.26.453836.

Dilks, C.M., Hahnel, S.R., Sheng, Q., Long, L., McGrath, P.T., Andersen, E.C., 2020. Quantitative benzimidazole resistance and fitness effects of parasitic nematode beta-tubulin alleles. Int. J. Parasitol. Drugs Drug Resist. 14, 28–36.

Doyle, S.R., Cotton, J.A., 2019. Genome-wide approaches to investigate anthelmintic resistance. Trends Parasitol. 35 (4), 289–301.

Doyle, S.R., Laing, R., Bartley, D., Morrison, A., Holroyd, N., Maitland, K., Antonopoulos, A., Chaudhry, U., Flis, I., Howell, S., McIntyre, J., Gilleard, J.S., Tait, A., Mable, B., Kaplan, R., Sargison, N., Britton, C., Berriman, M., Devaney, E., Cotton, J.A., 2022. Genomic landscape of drug response reveals novel mediators of anthelmintic resistance. bioRxiv. https://doi.org/10.1101/2021.11.12.465712.

Doyle, S.R., Illingworth, C.J.R., Laing, R., Bartley, D.J., Redman, E., Martinelli, A., Holroyd, N., Morrison, A.A., Rezansoff, A., Tracey, A., Devaney, E., Berriman, M., Sargison, N., Cotton, J.A., Gilleard, J.S., 2019. Population genomic and evolutionary modelling analyses reveal a single major QTL for ivermectin drug resistance in the pathogenic nematode, *Haemonchus contortus*. BMC Genomics 20, 218.

Doyle, S.R., Tracey, A., Laing, R., Holroyd, N., Bartley, D., Bazant, W., Beasley, H., Beech, R., Britton, C., Brooks, K., Chaudhry, U., Maitland, K., Martinelli, A., Noonan, J.D., Paulini, M., Quail, M.A., Redman, E., Rodgers, F.H., Sallé, G., Shabbir, M.Z., Sankaranarayanan, G., Wit, J., Howe, K.L., Sargison, N., Devaney, E., Berriman, M., Gilleard, J.S., Cotton, J.A., 2020. Genomic and transcriptomic variation defines the chromosome-scale assembly of *Haemonchus contortus*, a model gastrointestinal worm. Commun. Biol. 3, 656.

Furtado, L.F.V., Medeiros, C.d.S., Zuccherato, L.W., Alves, W.P., de Oliveira, V.N.G.M., da Silva, V.J., Miranda, G.S., Fujiwara, R.T., Rabelo, É.M.L., Churcher, T.S., 2019. First identification of the benzimidazole resistance-associated F200Y SNP in the beta-tubulin gene in *Ascaris lumbricoides*. PLoS One 14, (10) e0224108.

Gilleard, J.S., 2006. Understanding anthelmintic resistance: the need for genomics and genetics. Int. J. Parasitol. 36 (12), 1227–1239.

Gilleard, J.S., 2013. *Haemonchus contortus* as a paradigm and model to study anthelmintic drug resistance. Parasitology 140 (12), 1506–1522.

Gilleard, J.S., Redman, E., 2016. Genetic Diversity and Population Structure of Haemonchus contortus. Haemonchus contortus and Haemonchosis – Past, Present and Future Trends. Adv. Parasitol. 93, 31–68. https://doi.org/10.1016/bs.apar.2016.02.009.

Glendinning, S.K., Buckingham, S.D., Sattelle, D.B., Wonnacott, S., Wolstenholme, A. J., Carlow, C.K.S., 2011. Glutamate-gated chloride channels of *Haemonchus contortus* restore drug sensitivity to ivermectin resistant *Caenorhabditis elegans*. PLoS One 6, (7) e22390.

Graham, C.F., Boreham, D.R., Manzon, R.G., Stott, W., Wilson, J.Y., Somers, C.M., Feltus, F.A., 2020. How "simple" methodological decisions affect interpretation of population structure based on reduced representation library DNA sequencing: A case study using the lake whitefish. PLoS One 15, (1) e0226608.

Guest, M., Bull, K., Walker, R.J., Amliwala, K., O'Connor, V., Harder, A., Holden-Dye, L., Hopper, N.A., 2007. The calcium-activated potassium channel, SLO-1, is required for the action of the novel cyclo-octadepsipeptide anthelmintic, emodepside, in *Caenorhabditis elegans*. Int. J. Parasitol. 37, 1577–1588.

Hahnel, S.R., Zdraljevic, S., Rodriguez, B.C., Zhao, Y., McGrath, P.T., Andersen, E.C., 2018. Extreme allelic heterogeneity at a *Caenorhabditis elegans* beta-tubulin locus explains natural resistance to benzimidazoles. PLoS Pathog. 14, e1007226.

Hohenlohe, P.A., Bassham, S., Etter, P.D., Stiffler, N., Johnson, E.A., Cresko, W.A., 2010. Population genomics of parallel adaptation in threespine stickleback using sequenced RAD tags. PLoS Genet. 6, e1000862.

Houston, R.D., Bean, T.P., Macqueen, D.J., Gundappa, M.K., Jin, Y.H., Jenkins, T.L., Selly, S.L.C., Martin, S.A.M., Stevens, J.R., Santos, E.M., Davie, A., Robledo, D., 2020. Harnessing genomics to fast-track genetic improvement in aquaculture. Nat. Rev. Genet. 21, 389–409.

Hunt, V.L., Tsai, I.J., Coghlan, A., Reid, A.J., Holroyd, N., Foth, B.J., Tracey, A., Cotton, J. A., Stanley, E.J., Beasley, H., et al., 2016. The genomic basis of parasitism in the Strongyloides clade of nematodes. Nat. Genet. 48, 299–307.

Hunt, P.W., Kotze, A.C., Knox, M.R., Anderson, L.J., McNally, J., Jambre, L.E., 2010. The use of DNA markers to map anthelmintic resistance loci in an intraspecific cross of *Haemonchus contortus*. Parasitology 137, 705–717.

Jacobsen, M.W., Pujolar, J.M., Bernatchez, L., Munch, K., Jian, J., Niu, Y., Hansen, M.M., 2014. Genomic footprints of speciation in Atlantic eels (*Anguilla anguilla* and *A. rostrata*). Mol. Ecol. 23, 4785–4798.

Janssen, I.J.I., Krücken, J., Demeler, J., Basiaga, M., Kornaś, S., von Samson-Himmelstjerna, G., 2013. Genetic variants and increased expression of *Parascaris equorum* P-glycoprotein-11 in populations with decreased ivermectin susceptibility. PLoS One 8, e61635.

Jombart, T., Ahmed, I., 2011. adegenet 1.3-1: new tools for the analysis of genome-wide SNP data. Bioinformatics 27, 3070–3071.

Kaminsky, R., Ducray, P., Jung, M., Clover, R., Rufener, L., Bouvier, J., Weber, S.S., Wenger, A., Wieland-Berghausen, S., Goebel, T., Gauvry, N., Pautrat, F., Skripsky, T., Froelich, O., Komoin-Oka, C., Westlund, B., Sluder, A., Mäser, P., 2008. A new class of anthelmintics effective against drug-resistant nematodes. Nature 452, 176–180.

Kaplan, R.M., Vidyashankar, A.N., 2012. An inconvenient truth: global worming and anthelmintic resistance. Vet. Parasitol. 186, 70–78.

Khan, S., Zhao, X., Hou, Y., Yuan, C., Li, Y., Luo, X., Liu, J., Feng, X., 2019. Analysis of genome-wide SNPs based on 2b-RAD sequencing of pooled samples reveals signature of selection in different populations of *Haemonchus contortus*. J. Biosci. 44 (4), 1–13.

Knaus, B.J., Grünwald, N.J., 2017. vcfr: a package to manipulate and visualize variant call format data in R. Mol. Ecol. Resour. 17, 44–53.

Kofler, R., Orozco-terWengel, P., De Maio, N., Pandey, R.V., Nolte, V., Futschik, A., Kosiol, C., Schlötterer, C., 2011a. PoPoolation: a toolbox for population genetic analysis of next generation sequencing data from pooled individuals. PLoS One 6, e15925.

Kofler, R., Pandey, R.V., Schlötterer, C., 2011b. PoPoolation2: identifying differentiation between populations using sequencing of pooled DNA samples (Pool-Seq). Bioinformatics 27, 3435–3436.

Kotze, A.C., Gilleard, J.S., Doyle, S.R., Prichard, R.K., 2020. Challenges and opportunities for the adoption of molecular diagnostics for anthelmintic resistance. Int. J. Parasitol. Drugs Drug Resist. 14, 264–273.

Krücken, J., Fraundorfer, K., Mugisha, J.C., Ramünke, S., Sifft, K.C., Geus, D., Habarugira, F., Ndoli, J., Sendegeya, A., Mukampunga, C., Bayingana, C., Aebischer, T., Demeler, J., Gahutu, J.B., Mockenhaupt, F.P., von Samson-Himmelstjerna, G., 2017. Reduced efficacy of albendazole against *Ascaris lumbricoides* in Rwandan schoolchildren. Int. J. Parasitol. Drugs Drug Resist. 7, 262–271.

Kumar, G., Kocour, M., 2017. Applications of next-generation sequencing in fisheries research: A review. Fish. Res. 186, 11–22.

Kwa, M.S.G., Veenstra, J.G., Roos, M.H., 1993. Molecular characterisation of β-tubulin genes present in benzimidazole-resistant populations of *Haemonchus contortus*. Mol. Biochem. Parasitol. 60, 133–143.

Kwa, M.S.G., Veenstra, J.G., Roos, M.H., 1994. Benzimidazole resistance in *Haemonchus contortus* is correlated with a conserved mutation at amino acid 200 in β-tubulin isotype 1. Mol. Biochem. Parasitol. 63, 299–303.

Kwa, M.S.G., Veenstra, J.G., Van Dijk, M., Roos, M.H., 1995. β-tubulin genes from the parasitic nematode *Haemonchus contortus* modulate drug resistance in *Caenorhabditis elegans*. J. Mol. Biol. 246, 500–510.

Laing, R., Kikuchi, T., Martinelli, A., Tsai, I.J., Beech, R.N., Redman, E., Holroyd, N., Bartley, D.J., Beasley, H., Britton, C., Curran, D., Devaney, E., Gilabert, A., Hunt, M., Jackson, F., Johnston, S.L., Kryukov, I., Li, K., Morrison, A.A., Reid, A.J., Sargison, N., Saunders, G.I., Wasmuth, J.D., Wolstenholme, A., Berriman, M., Gilleard, J.S., Cotton, J.A., 2013. The genome and transcriptome of *Haemonchus contortus*, a key model parasite for drug and vaccine discovery. Genome Biol. 14, R88.

Laing, R., Doyle, S.R., McIntyre, J., Maitland, K., Morrison, A., Bartley, D.J., Kaplan, R., Chaudhry, U., Sargison, N., Tait, A., Cotton, J.A., Britton, C., Devaney, E., 2022. Transcriptomic analyses implicate neuronal plasticity and chloride homeostasis in ivermectin resistance and response to treatment in a parasitic nematode. PLoS Pathogens 18 (6), e1010545.

Langmead, B., Salzberg, S.L., 2012. Fast gapped-read alignment with Bowtie 2. Nat. Methods 9, 357–359.

Le Jambre, L.F., Gill, J.H., Lenane, I.J., Baker, P., 2000. Inheritance of avermectin resistance in *Haemonchus contortus*. Int. J. Parasitol. 30, 105–111.

Lepais, O., Weir, J.T., 2014. SimRAD: an R package for simulation-based prediction of the number of loci expected in RAD-seq and similar genotyping by sequencing approaches. Mol. Ecol. Resour. 14, 1314–1321.

Li, H., Handsaker, B., Wysoker, A., Fennell, T., Ruan, J., Homer, N., Marth, G., Abecasis, G., Durbin 1000 Genome Project Data Processing Subgroup, R., 2009. The Sequence Alignment/Map format and SAMtools. Bioinformatics 25 (16), 2078–2079.

Łopieńska-Biernat, E., Paukszto, Ł., Jastrzębski, J.P., Myszczyński, K., Polak, I., Stryiński, R., 2019. Genome-wide analysis of *Anisakis simplex* sensu lato: the role of carbohydrate metabolism genes in the parasite's development. Int. J. Parasitol. 49, 933–943.

Lowry, D.B., Hoban, S., Kelley, J.L., Lotterhos, K.E., Reed, L.K., Antolin, M.F., Storfer, A., 2017a. Responsible RAD: Striving for best practices in population genomic studies of adaptation. Mol. Ecol. Resour. 17 (3), 366–369.

Lowry, D.B., Hoban, S., Kelley, J.L., Lotterhos, K.E., Reed, L.K., Antolin, M.F., Storfer, A., 2017b. Breaking RAD: an evaluation of the utility of restriction site-associated DNA sequencing for genome scans of adaptation. Mol. Ecol. Resour. 17, 142–152.

Luo, X., Shi, X., Yuan, C., Ai, M., Ge, C., 2017. Genome-wide SNP analysis using 2b-RAD sequencing identifies the candidate genes putatively associated with resistance to ivermectin in *Haemonchus contortus*. Parasit. Vectors 10 (1), 1–10.

Lynch, M., Bost, D., Wilson, S., Maruki, T., Harrison, S., 2014. Population-genetic inference from pooled-sequencing data. Genome Biol. Evol. 6, 1210–1218.

Martin, M., 2011. Cutadapt removes adapter sequences from high-throughput sequencing reads. EMBnet.journal 17, 10–12.

Matoušková, P., Lecová, L., Laing, R., Dimunová, D., Vogel, H., Raisová Stuchlíková, L., Nguyen, L.T., Kellerová, P., Vokřál, I., Lamka, J., Szotáková, B., Várady, M., Skálová, L., 2018. UDP-glycosyltransferase family in *Haemonchus contortus*: phylogenetic analysis, constitutive expression, sex-differences and resistance-related differences. Int. J. Parasitol. Drugs Drug Resist. 8, 420–429.

McCavera, S., Rogers, A.T., Yates, D.M., Woods, D.J., Wolstenholme, A.J., 2009. An ivermectin-sensitive glutamate-gated chloride channel from the parasitic nematode *Haemonchus* contortus. Mol. Pharmacol. 75, 1347–1355.

McKinney, G.J., Larson, W.A., Seeb, L.W., Seeb, J.E., 2017. RAD-seq provides unprecedented insights into molecular ecology and evolutionary genetics: comment on Breaking RAD by Lowry et al. (2016). Mol. Ecol. Resour. 17(3), 356-361.

Mutombo, P.N., Man, N.W.Y., Nejsum, P., Ricketson, R., Gordon, C.A., Robertson, G., Clements, A.C.A., Chacón-Fonseca, N., Nissapatorn, V., Webster, J.P., McLaws, M.-L., 2019. Diagnosis and drug resistance of human soil-transmitted helminth infections: A public health perspective. Adv. Parasitol. 104, 247–326.

Orr, A.R., Quagraine, J.E., Suwondo, P., George, S., Harrison, L.M., Dornas, F.P., Evans, B., Caccone, A., Humphries, D., Wilson, M.D., Cappello, M., 2019. Genetic Markers of Benzimidazole Resistance among Human Hookworms (*Necator americanus*) in Kintampo North Municipality. Ghana. Am. J. Trop. Med. Hyg. 100, 351–356.

Paradis, E., 2010. pegas: an R package for population genetics with an integrated–modular approach. Bioinformatics 26, 419–420.

Paradis, E., Claude, J., Strimmer, K., 2004. APE: Analyses of Phylogenetics and Evolution in R language. Bioinformatics 20, 289–290.

Peterson, B.K., Weber, J.N., Kay, E.H., Fisher, H.S., Hoekstra, H.E., 2012. Double digest RAD-seq: an inexpensive method for de novo SNP discovery and genotyping in model and non-model species. PLoS One 7, e37135.

Prichard, R., 2001. Genetic variability following selection of *Haemonchus contortus* with anthelmintics. Trends Parasitol. 17, 445–453.

Prichard, R.K., Roulet, A., 2007. ABC transporters and beta-tubulin in macrocyclic lactone resistance: prospects for marker development. Parasitology 134, 1123–1132.

Puritz, J.B., Matz, M.V., Toonen, R.J., Weber, J.N., Bolnick, D.I., Bird, C.E., 2014. Demystifying the RAD fad. Mol. Ecol. 23, 5937–5942.

Quinlan, A.R., 2014. BEDTools: the Swiss-army tool for genome feature analysis. Curr. Protoc. Bioinformatics 47, 11–12.

Quinlan, A.R., Hall, I.M., 2010. BEDTools: a flexible suite of utilities for comparing genomic features. Bioinformatics 26, 841–842.

Redman, E., Grillo, V., Saunders, G., Packard, E., Jackson, F., Berriman, M., Gilleard, J. S., 2008. Genetics of mating and sex determination in the parasitic nematode *Haemonchus contortus*. Genetics 180, 1877–1887.

Redman, E., Sargison, N., Whitelaw, F., Jackson, F., Morrison, A., Bartley, D.J., Gilleard, J.S., 2012. Introgression of ivermectin resistance genes into a susceptible *Haemonchus contortus* strain by multiple backcrossing. PLoS Pathog. 8, e1002534.

Rezansoff, A.M., Laing, R., Martinelli, A., Stasiuk, S., Redman, E., Bartley, D., Holroyd, N., Devaney, E., Sargison, N.D., Doyle, S., Cotton, J.A., Gilleard, J.S., 2019. The confounding effects of high genetic diversity on the determination and interpretation of differential gene expression analysis in the parasitic nematode *Haemonchus contortus*. Int. J. Parasitol. 49, 847–858.

Rose Vineer, H., Morgan, E.R., Hertzberg, H., Bartley, D.J., Bosco, A., Charlier, J., Chartier, C., Claerebout, E., de Waal, T., Hendrickx, G., Hinney, B., Höglund, J., Ježek, J., Kašný, M., Keane, O.M., Martínez-Valladares, M., Mateus, T.L., McIntyre, J., Mickiewicz, M., Munoz, A.M., Phythian, C.J., Ploeger, H.W., Rataj, A.V., Skuce, P.J., Simin, S., Sotiraki, S., Spinu, M., Stuen, S., Thamsborg, S.M., Vadlejch, J., Varady, M., von Samson-Himmelstjerna, G., Rinaldi, L., 2020. Increasing importance of anthelmintic resistance in European livestock: creation and meta-analysis of an open database. Parasite 27, 69.

Rufener, L., Mäser, P., Roditi, I., Kaminsky, R., 2009. *Haemonchus contortus* acetylcholine receptors of the DEG-3 subfamily and their role in sensitivity to monepantel. PLoS Pathog. 5, e1000380.

Sallé, G., Doyle, S.R., Cortet, J., Cabaret, J., Berriman, M., Holroyd, N., Cotton, J.A., 2019. The global diversity of *Haemonchus contortus* is shaped by human intervention and climate. Nat. Commun. 10, 4811.

Schloss, P.D., Westcott, S.L., Ryabin, T., Hall, J.R., Hartmann, M., Hollister, E.B., Lesniewski, R.A., Oakley, B.B., Parks, D.H., Robinson, C.J., Sahl, J.W., Stres, B., Thallinger, G.G., Van Horn, D.J., Weber, C.F., 2009. Introducing mothur: open-source, platform-independent, community-supported software for describing and comparing microbial communities. Appl. Environ. Microbiol. 75, 7537–7541.

Settepani, V., Schou, M.F., Greve, M., Grinsted, L., Bechsgaard, J., Bilde, T., 2017. Evolution of sociality in spiders leads to depleted genomic diversity at both population and species levels. Mol. Ecol. 26, 4197–4210.

Tinkler, S.H., 2020. Preventive chemotherapy and anthelmintic resistance of soil-transmitted helminths - Can we learn nothing from veterinary medicine? One Health 9, 100106.

Urdaneta-Marquez, L., Bae, S.H., Janukavicius, P., Beech, R., Dent, J., Prichard, R., 2014. A dyf-7 haplotype causes sensory neuron defects and is associated with macrocyclic lactone resistance worldwide in the nematode parasite *Haemonchus contortus*. Int. J. Parasitol. 44, 1063–1071.

Valentim, C.L.L., Cioli, D., Chevalier, F.D., Cao, X., Taylor, A.B., Holloway, S.P., Pica-Mattoccia, L., Guidi, A., Basso, A., Tsai, I.J., Berriman, M., Carvalho-Queiroz, C., Almeida, M., Aguilar, H., Frantz, D.E., Hart, P.J., LoVerde, P.T., Anderson, T.J.C., 2013. Genetic and molecular basis of drug resistance and species-specific drug action in schistosome parasites. Science 342, 1385–1389.

Wit, J., Dilks, C.M., Andersen, E.C., 2021. Complementary approaches with free-living and parasitic nematodes to understanding anthelmintic resistance. Trends Parasitol. 37, 240–250.

Wit, J., Gilleard, J.S., 2017. Resequencing helminth genomes for population and genetic studies. Trends Parasitol. 33, 388–399.

Wright, B.R., Farquharson, K.A., McLennan, E.A., Belov, K., Hogg, C.J., Grueber, C.E., 2020. A demonstration of conservation genomics for threatened species management. Mol. Ecol. Resour. 20, 1526–1541.

Yeaman, S., Hodgins, K.A., Lotterhos, K.E., Suren, H., Nadeau, S., Degner, J.C., Nurkowski, K.A., Smets, P., Wang, T., Gray, L.K., Liepe, K.J., Hamann, A., Holliday, J.A., Whitlock, M.C., Rieseberg, L.H., Aitken, S.N., 2016. Convergent local adaptation to climate in distantly related conifers. Science 353, 1431–1433.

Zamanian, M., Cook, D.E., Zdraljevic, S., Brady, S.C., Lee, D., Lee, J., Andersen, E.C., 2018. Discovery of genomic intervals that underlie nematode responses to benzimidazoles. PLoS Negl. Trop. Dis. 12.